

# Effect of $\rho N$ channel in the $\gamma N \rightarrow \pi\pi N$ reactions

M. Hirata<sup>\*</sup>, K. Ochi<sup>†</sup>

*Department of Physics, Hiroshima University, Higashi-Hiroshima 739, Japan*

and

T. Takaki<sup>‡</sup>

*Onomichi Junior College, Onomichi 722, Japan*

## Abstract

A model for the two-pion photoproduction on the nucleon proposed earlier is modified to simultaneously explain the total cross sections and the invariant mass spectra. Using this model, we discuss the role of the  $\rho$  meson in the  $\gamma N \rightarrow \pi\pi N$  reaction.

PACS number(s): 25.20.Lj, 25.20.Dc, 13.60.Rj

---

<sup>\*</sup>E-mail: hirata@theo.phys.sci.hiroshima-u.ac.jp

<sup>†</sup>E-mail: kazu@theo.phys.sci.hiroshima-u.ac.jp

<sup>‡</sup>E-mail: takaki@hiroshima-cdas.or.jp

Recently, the two-pion photoproduction on the nucleon have been experimentally studied for the photon energy from 450 to 800 MeV at Mainz Microtron MAMI [1–3]. The total cross sections of the  $\gamma p \rightarrow \pi^+\pi^0 n$  and  $\gamma p \rightarrow \pi^0\pi^0 p$  reactions have been obtained for the first time using the large acceptance detector DAPHNE and high intensity tagged photon beams [1,2]. The  $\gamma p \rightarrow \pi^+\pi^- p$  and  $\gamma n \rightarrow \pi^-\pi^0 p$  cross sections have been also measured with good accuracy. Then,  $\gamma p \rightarrow \pi^0\pi^0 p$  cross sections have been measured using the Glasgow Tagger and the TAPS photon spectrometer [3] and the previous experimental result has been confirmed. A characteristic feature in this energy region is that the resonances such as  $\Delta(1232)$  and  $N^*(1520)$  are involved in the production process.

DAPHNE-experiments have motivated several authors [4–6] to develop the model for the  $\gamma N \rightarrow \pi\pi N$  reaction. The theoretical studies for the  $\gamma p \rightarrow \pi^+\pi^- p$  reaction have shown that the two-pion photoproduction takes place dominantly through the  $\pi\Delta(1232)$  intermediate state, which arises from the  $\Delta$  Kroll-Ruderman and  $\Delta$  pion-pole terms [Figs. 1(a)-1(b)] and the  $N^*(1520)$  excitation [Fig. 1(c)]. The interference between the  $\Delta$  Kroll-Ruderman and the  $N^*(1520)$  excitation processes is essential to reproduce the energy dependence of the total cross section [4].

However, it has been found that the neutral pion production such as the  $\gamma p \rightarrow \pi^+\pi^0 n$  and  $\gamma n \rightarrow \pi^-\pi^0 p$  cannot be explained with only the  $\pi\Delta(1232)$  production mechanism which dominates the  $\gamma p \rightarrow \pi^+\pi^- p$  reaction and therefore some additional mechanism is needed. In fact, the magnitude of cross sections is largely underestimated compared with the data [4,5]. In our previous paper [6], we have proposed a simple model which is able to explain the data and indicated that the  $\rho N$  intermediate state arising from both the  $N^*(1520)$  excitation [Fig. 1(d)] and the  $\rho$  Kroll-Ruderman process [Fig. 1(e)] plays an important role in the  $\gamma p \rightarrow \pi^+\pi^0 n$  and  $\gamma n \rightarrow \pi^-\pi^0 p$  reactions.

We note that the transitions to the  $\pi\Delta$  channel in these reactions, especially the  $\Delta$  Kroll-Ruderman and  $\Delta$  pion-pole processes, are suppressed compared with the  $\gamma p \rightarrow \pi^+\pi^- p$  reaction because of the isospin factors.

In addition to the total cross sections of the two-pion photoproduction, the measurements of the invariant mass spectra on the  $\gamma n \rightarrow \pi^-\pi^0 p$  reaction have been performed at Mainz lately [7]. This experimental result can provide an additional constraint on the theoretical model. In this letter, we report a modified version of our model and discuss our results concerning the total cross sections and the invariant mass spectra.

First of all, we review the formalism of our model briefly [6]. The  $T$  matrix for the two-pion photoproduction is written as

$$T = T_{\Delta KR} + T_{\Delta PP} + T_{N^*\pi\Delta}^s + T_{N^*\pi\Delta}^d + T_{N^*\rho N} + T_{\rho KR}. \quad (1)$$

The  $T$  matrix includes two dominant channels, i.e., the  $\pi\Delta(1232)$  and  $\rho N$  channels. These states are assumed to arise from six processes described by the  $\Delta$  Kroll-Ruderman term ( $T_{\Delta KR}$ ),  $\Delta$  pion-pole term ( $T_{\Delta PP}$ ),  $N^*(1520)$  excitation terms ( $T_{N^*\pi\Delta}^{s(d)}$  and  $T_{N^*\rho N}$ ), and  $\rho$  Kroll-Ruderman term ( $T_{\rho KR}$ ) which are shown in Figs. 1 (a)-(e), respectively. The  $N^*(1520)$  decay into a  $\pi\pi N$  occurs through three channels: the  $s$ -wave  $\pi\Delta(1232)$ ,  $d$ -wave  $\pi\Delta(1232)$  and  $\rho N$  channels. The branching fractions into these decay channels are comparable.

The  $\Delta$  Kroll-Ruderman and  $\Delta$  pion-pole terms are written as

$$T_{\Delta KR} = F_{\pi N\Delta} G_{\pi\Delta}(s, \vec{p}_\Delta) F_{\Delta KR}^\dagger, \quad (2)$$

$$T_{\Delta PP} = F_{\pi N\Delta} G_{\pi\Delta}(s, \vec{p}_\Delta) F_{\Delta PP}^\dagger, \quad (3)$$

where

$$G_{\pi\Delta}(s, \vec{p}_\Delta) = \frac{1}{\sqrt{s} - \omega_\pi(\vec{p}_\Delta) - E_\Delta(\vec{p}_\Delta) - \Sigma_\Delta^{(\pi N)}(s, \vec{p}_\Delta)}. \quad (4)$$

Here,  $F_{\pi N\Delta}$  is the  $\pi N\Delta$  vertex function which is taken to be the same vertex function used in the Betz-Lee model [8].  $G_{\pi\Delta}(s, \vec{p}_\Delta)$  is the propagator of the  $\pi\Delta$  system,  $\Sigma_\Delta^{(\pi N)}(s, \vec{p}_\Delta)$  is the  $\Delta$  self-energy with the momentum  $\vec{p}_\Delta$ , and  $\omega_\pi(\vec{p}_\Delta)$  and  $E_\Delta(\vec{p}_\Delta)$  are the energies of pion and  $\Delta$ , respectively.  $F_{\Delta KR}^\dagger$  is the  $\Delta$  Kroll-Ruderman vertex which are obtained from the  $N \rightarrow \pi\Delta$  vertex function by requiring gauge invariance. This  $N \rightarrow \pi\Delta$  vertex function is assumed to be the same form with the  $\Delta \rightarrow \pi N$  vertex function of the Betz-Lee model. The range parameter of the form factor  $Q_\Delta(N \rightarrow \pi\Delta)$  is, however, varied and determined to fit the  $\gamma p \rightarrow \pi^+\pi^-p$  cross section.  $F_{\Delta PP}^\dagger$  is the  $\Delta$  pion-pole vertex. The  $N^*(1520)$  terms are written as

$$T_{N^*\pi\Delta}^{s(d)} = F_{\pi N\Delta} G_{\pi\Delta}(s, \vec{p}_\Delta) F_{\pi\Delta N^*}^{s(d)} G_{N^*}(s) \tilde{F}_{\gamma NN^*}^\dagger, \quad (5)$$

$$T_{N^*\rho N} = F_{\rho\pi\pi} G_{\rho N}(s, \vec{q}_\rho) F_{\rho NN^*} G_{N^*}(s) \tilde{F}_{\gamma NN^*}^\dagger, \quad (6)$$

where

$$G_{N^*}(s) = \frac{1}{\sqrt{s} - M_{N^*} - \Sigma_{N^*}(s)}, \quad (7)$$

$$G_{\rho N}(s, \vec{q}_\rho) = \frac{1}{2\omega_\rho(\vec{q}_\rho)[\sqrt{s} - \omega_\rho(\vec{q}_\rho) - E_N(\vec{q}_\rho) - \Sigma_{\rho\pi\pi}(s, \vec{q}_\rho)]}. \quad (8)$$

Here,  $\tilde{F}_{\gamma NN^*}^\dagger$  is the  $\gamma NN^*$  vertex function.  $F_{\pi\Delta N^*}^{s(d)}$  is the  $\pi\Delta N^*$  vertex function for the  $s$ - or  $d$ -wave  $\pi\Delta$  state and  $F_{\rho NN^*}$  is the  $\rho NN^*$  vertex function, respectively.  $F_{\rho\pi\pi}$  is the  $\rho\pi\pi$  vertex function.  $G_{N^*}(s)$  and  $G_{\rho N}(s, \vec{q}_\rho)$  are the propagators of the  $N^*(1520)$  and  $\rho N$  system, respectively.  $\Sigma_{N^*}(s)$  is the  $N^*$  self-energy in the center of mass system and  $\Sigma_{\rho\pi\pi}(s, \vec{q}_\rho)$  is the  $\rho$  meson self-energy with the momentum  $\vec{q}_\rho$ .  $M_{N^*}$  is the bare mass of  $N^*$  and  $\omega_\rho(\vec{q}_\rho)$  and  $E_N(\vec{q}_\rho)$  are the energies of the  $\rho$  meson and nucleon, respectively. The  $\rho$  Kroll-Ruderman term is written as

$$T_{\rho KR} = F_{\rho\pi\pi} G_{\rho N}(s, \vec{q}_\rho) F_{\rho KR}^\dagger, \quad (9)$$

where  $F_{\rho KR}$  is the  $\rho$  Kroll-Ruderman vertex which is derived from the non-relativistic  $\rho NN$  vertex function by requiring gauge invariance. The detailed forms of the above vertex functions are given in Ref. [6]. The self-energies of the  $N^*$ ,  $\pi\Delta$  system and  $\rho N$  system in the propagators are obtained by using these strong vertex functions whose expressions are also given in Ref. [6].

Most of the parameters such as coupling constants, range parameters and bare masses are phenomenologically obtained by using the  $\pi N$  scattering amplitudes,  $\gamma N \rightarrow \pi N$  multipole amplitudes, branching fractions of the  $N^*(1520)$  and width of the  $\rho$ -meson, but the signs of the coupling constants and the range parameters such as  $Q_\Delta(N \rightarrow \pi\Delta)$  and  $q_{\rho\pi\pi}$  are not determined. Here  $q_{\rho\pi\pi}$  is the range parameter of the  $\rho\pi\pi$  form factor. The  $\gamma N \rightarrow \pi\pi N$  reaction data is necessary to fix the signs and these remaining parameters. In order to fix these parameters, we took the following way: The signs of the coupling constants and the

range parameter  $Q_\Delta(N \rightarrow \pi\Delta)$  were determined so as to reproduce the  $\gamma p \rightarrow \pi^+\pi^-p$  cross section. The range parameter  $q_{\rho\pi\pi}$  was varied to fit the  $\gamma p \rightarrow \pi^+\pi^0n$  cross section, since the  $\rho N$  channel contributes to the  $\gamma p \rightarrow \pi^+\pi^0n$  more significantly than the  $\gamma p \rightarrow \pi^+\pi^-p$ . Then the cross sections in other isospin channels were calculated using the fixed parameters. The parameters determined in this way are given in Table 1.

With this parameter set, the total cross sections of  $\gamma N \rightarrow \pi\pi N$  can be almost reproduced except the high energy region of the  $\gamma p \rightarrow \pi^+\pi^0n$  and  $\gamma n \rightarrow \pi^-\pi^0p$  cross sections and the magnitude of the  $\gamma p \rightarrow \pi^0\pi^0p$  cross section. The calculated cross sections (dashed lines) of  $\gamma p \rightarrow \pi^+\pi^-p$ ,  $\gamma p \rightarrow \pi^+\pi^0n$  and  $\gamma n \rightarrow \pi^-\pi^0p$  are shown in Fig. 2.

The signs of the coupling constants such as  $f_{\pi\Delta N^*}^s > 0$ ,  $f_{\pi\Delta N^*}^d < 0$  and  $f_{\rho NN^*} < 0$  were necessary to explain the energy dependence of the  $\gamma p \rightarrow \pi^+\pi^-p$  cross section. The sign of  $f_{\pi\Delta N^*}^s$  should be positive to get the constructive interference between  $T_{\Delta KR}$  and  $T_{N^*\pi\Delta}^s$  below the resonance energy of  $N^*(1520)$  [4]. The negative sign of  $f_{\rho NN^*}$  was also necessary to simultaneously reproduce the cross sections for all isospin channels of  $\gamma N \rightarrow \pi\pi N$  reactions. As far as the total cross sections are concerned, the results of our model have been almost satisfactory except the double neutral pion photoproduction.

The recent experiment on the invariant mass spectra of the  $\gamma n \rightarrow \pi^-\pi^0p$  reaction [7] provides an opportunity to test the validity of our model and whether the determined parameters are appropriate or not. Although the data have not been published yet since they are still preliminary, there seem to be two interesting features from a qualitative point of view: the first one is the strong correlation at the larger invariant mass region in the invariant mass spectra of the  $(\pi\pi)$  system and the second one is the strong signal of the  $\Delta$  resonance in the invariant mass spectra of the  $(\pi N)$  system. We have calculated the invariant mass spectra with the parameter-set obtained previously and the results (dotted lines) at 730 MeV are shown in Figs. 3(a)-3(b). In the  $(\pi\pi)$  invariant mass spectrum [see Fig. 3(a)], we find that there are a strong peak and small bump coming from  $\rho N$  production compared with a uniform phase space distribution (thin solid line).

However, there are no such two peaks in the experimental spectrum [7]. The theoretical result does not qualitatively agree with the experiment. In this calculation, the bump at the small invariant mass is due to the  $\rho$  Kroll-Ruderman term and the peak at the large invariant mass is related to the  $N^*$  production following the decay to the  $\rho N$  system. To further investigate the origin of this discrepancy, we have also calculated the invariant mass spectrum of the  $(\pi\pi)$  system for the  $\gamma p \rightarrow \pi^+\pi^-p$  reaction at 750 MeV [see the dotted line in Fig. 3(c)]. Again, we find a strong peak at the large invariant mass which was not observed in the experimental spectrum [9]. This peak is caused by the constructive interference between the  $T_{\Delta KR}$  and  $T_{N^*\rho N}$  terms. We note that the  $\rho$  Kroll-Ruderman term does not contribute to the  $\gamma p \rightarrow \pi^+\pi^-p$  reaction. These discrepancies indicate that the  $\rho NN^*$  coupling constant  $f_{\rho NN^*}$  should be changed from the negative value to the positive one and the  $\rho$  Kroll-Ruderman contribution is too large at the small invariant mass region.

Taking these results into consideration, we modify the parameters to reproduce the total cross sections of the  $\gamma p \rightarrow \pi^+\pi^-p$  and  $\gamma p \rightarrow \pi^+\pi^0n$  reactions. The parameter-set obtained is shown in Table 1, where the sign of  $f_{\rho NN^*}$  is positive and the range parameter  $q_{\rho\pi\pi}$  is taken to be larger than the previous one. With these parameters, the cross sections and the invariant mass spectra are calculated and the results are shown in Figs. 2 and 3, respectively. The full calculations (thick solid lines) are consistent with the data except the

magnitude of the  $\gamma n \rightarrow \pi^- \pi^0 p$  cross sections in the higher energy region. The contributions of the  $\pi\Delta$  channel(dashed lines), the  $\rho N$  channel arising from the  $N^*$  production (long dashed lines) and the  $\rho$  Kroll-Ruderman term (dash dotted lines) are also plotted in Fig.3, respectively. The calculated invariant mass spectra at the other photon energies seem to almost consistent with the data from a qualitative point of view. In the  $(\pi\pi)$  invariant mass spectrum for  $\gamma n \rightarrow \pi^- \pi^0 p$ , one can observe that the peak shifts to the larger invariant mass compared with that of the uniform phase space distribution[see Fig.3(a)]. This is due to the  $N^*$  production following the decay to the  $\rho N$  system. The strong peak at the  $\Delta$  resonance energy in the  $(p\pi^0)$  invariant mass spectrum [see Fig. 3(b)] can be seen in the calculation and is attributed to the strong transition into the  $\pi\Delta$  state. These features in our theoretical results are also found in the data [9]. Furthermore, the  $\rho$  Kroll-Ruderman term is necessary to reproduce the magnitude of the cross sections for the neutral pion production such as the  $\gamma p \rightarrow \pi^+ \pi^0 n$  and  $\gamma n \rightarrow \pi^- \pi^0 p$  reactions. In the calculations with the modified parameter-set, the diagram of Fig. 1(f) is also included. This diagram contributes to the  $\gamma p \rightarrow \pi^0 \pi^0 p$  cross section significantly and leads to the improvement of the calculation. We note that the  $\rho N$  intermediate state does not contribute to the double neutral pion photoproduction. Since the discussion regarding this isospin channel is beyond the scope of this letter, we will report the results elsewhere. For the other isospin channels, this diagram modifies the cross sections slightly.

Finally, we discuss the disagreement between the calculation and the data in the  $\gamma n \rightarrow \pi^- \pi^0 p$  cross section. In this experiment, the cross sections have been measured by using the detector with a smaller acceptance ( $\leq 50\%$ ) compared with other isospin channels [2]. The total cross sections have been obtained by extrapolating the data using either a uniform phase space distribution or the Murphy-Laget model [5]. Since the experimental invariant mass spectra are deviated from the pure phase space distribution and the latter model underestimates the magnitude of the cross sections, the extrapolation procedure may be questionable. To demonstrate this ambiguity, we calculate the cross section integrated over the acceptance of the detector and extrapolate it by using the uniform phase space distribution to get the total cross section. As is seen in Fig. 2(c), our extrapolated cross sections (dash dotted line) are in good agreement with the data.

We find that our model with the modified parameters can explain the total cross sections of the two-pion photoproduction except the  $\gamma n \rightarrow \pi^- \pi^0 p$  cross sections fairly well and reproduce the characteristic behavior as mentioned above in the invariant mass spectra. These results confirm our previous findings that the  $\rho N$  channel plays an important role in the two-pion photoproduction as well as the  $\pi\Delta$  channel, especially in the  $\gamma p \rightarrow \pi^+ \pi^0 n$  and  $\gamma n \rightarrow \pi^- \pi^0 p$  reactions. The experimental cross sections of the  $\gamma n \rightarrow \pi^- \pi^0 p$  reaction obtained by the extrapolation procedure are largely model-dependent as is inferred in the above discussion. In order to examine a theoretical model, one should compare the theory directly with the data integrated over the acceptance of the detector.

## ACKNOWLEDGMENTS

We thank Prof. P. Pedroni for providing us with the data collected at Mainz prior to publication.

## REFERENCES

- [1] A. Braghieri et al., Phys.Lett. B **363** (1995) 46.
- [2] A. Zabrodin et al., Phys. Rev. C **55** (1997) R1.
- [3] F. Härter et al., Phys. Lett. B **401** (1997) 229.
- [4] J. A. G. Tejedor and E. Oset, Nucl. Phys. **A 571** (1994) 667; Nucl. Phys. **A 600** (1997) 413.
- [5] L.Y. Murphy and J.M. Laget, DAPNIA/SPhN 95-42 (1995).
- [6] K. Ochi, M. Hirata, and T. Takaki, Phys. Rev. C **56** (1997) 1472.
- [7] P. Pedroni, private communication.
- [8] M. Betz and T.-S.H.Lee, Phys. Rev. C **23** (1981) 375.
- [9] Aachen-Berlin-Bonn-Hamburg-Heidelberg-München Collaboration, Phys. Rev. **175** (1968) 1669.
- [10] A. Piazza et al., Nuovo Cimento **III** (1970) 403.
- [11] F. Carbonara et al., Nuovo Cimento **36 A** (1976) 219.

# TABLES

TABLE I. The parameters used in our model. The old parameter-set corresponds to the parameter-set(II) in Ref. [6]. The definitions of the parameters are described in the text and Ref. [6]. (<sup>a</sup>This value is the sum of the vector and tensor coupling constants.)

	Old parameter-set	New parameter-set
$M_{N^*}(\text{MeV})$	1554	1566
$f_{\pi NN^*}$	1.13	1.13
$p_{\pi NN^*}(\text{MeV}/c)$	400	400
$f_{\pi\Delta N^*}^s$	0.992	0.992
$p_{\pi\Delta N^*}^s(\text{MeV}/c)$	200	200
$f_{\pi\Delta N^*}^d$	-1.00	-1.00
$p_{\pi\Delta N^*}^d(\text{MeV}/c)$	300	300
$f_{\rho NN^*}$	-0.928	0.583
$p_{\rho NN^*}(\text{MeV}/c)$	200	300
$f_{\rho\pi\pi}$	82.0	25.6
$q_{\rho\pi\pi}(\text{MeV}/c)$	100	200
$Q_{\Delta}(N \rightarrow \pi\Delta)(\text{MeV}/c)$	400	480
$Q_{\Delta}(\Delta \rightarrow \pi N)(\text{MeV}/c)$	358	358
$G_T$	17.6	21.05 <sup>a</sup>

## FIGURES

FIG. 1. Diagrams for the two-pion production. (a) The  $\Delta$  Kroll-Ruderman term. (b) The  $\Delta$  pion-pole term. (c) The  $N^* \rightarrow \pi\Delta$  contribution. (d) The  $N^* \rightarrow \rho N$  contribution. (e) The  $\rho$  Kroll-Ruderman term. (f) The  $\pi\Delta$  production accompanied by the nucleon exchange.

FIG. 2. The total cross sections of (a) the  $\gamma p \rightarrow \pi^+\pi^-p$ , (b)  $\gamma p \rightarrow \pi^+\pi^0n$  and (c)  $\gamma n \rightarrow \pi^-\pi^0p$  reactions. The solid lines are the calculations with a new parameter-set. The dashed lines are the calculations with an old parameter-set. The dash dotted line in the  $\gamma n \rightarrow \pi^-\pi^0p$  reaction is the extrapolated cross section(see the text for detail). Experimental data are taken from Refs. [1,2,9–11]

FIG. 3. The invariant mass spectra of (a) the  $(\pi^-\pi^0)$  and (b)  $(p\pi^0)$  systems for the  $\gamma n \rightarrow \pi^-\pi^0p$  reaction at 730 MeV and (c) the  $(\pi^+\pi^-)$  system for the  $\gamma p \rightarrow \pi^+\pi^-p$  reaction at 750MeV, respectively. The thick solid lines are the full calculations with a new parameter-set. The contributions of the  $\pi\Delta$  channel(dashed lines), the  $\rho N$  channel arising from the  $N^*$  production (long dashed lines) and the  $\rho$  Kroll-Ruderman term (dash dotted lines) are also plotted. The dotted lines are the full calculations with an old parameter-set. The calculated cross sections are obtained by integrating over all phase space. Experimental data [9] are appropriately normalized.



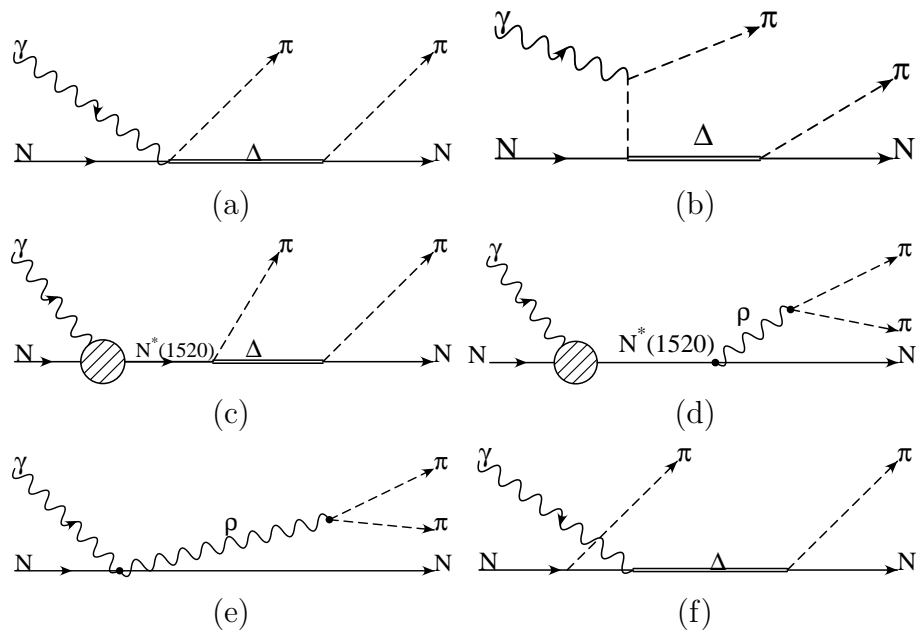


Figure 1

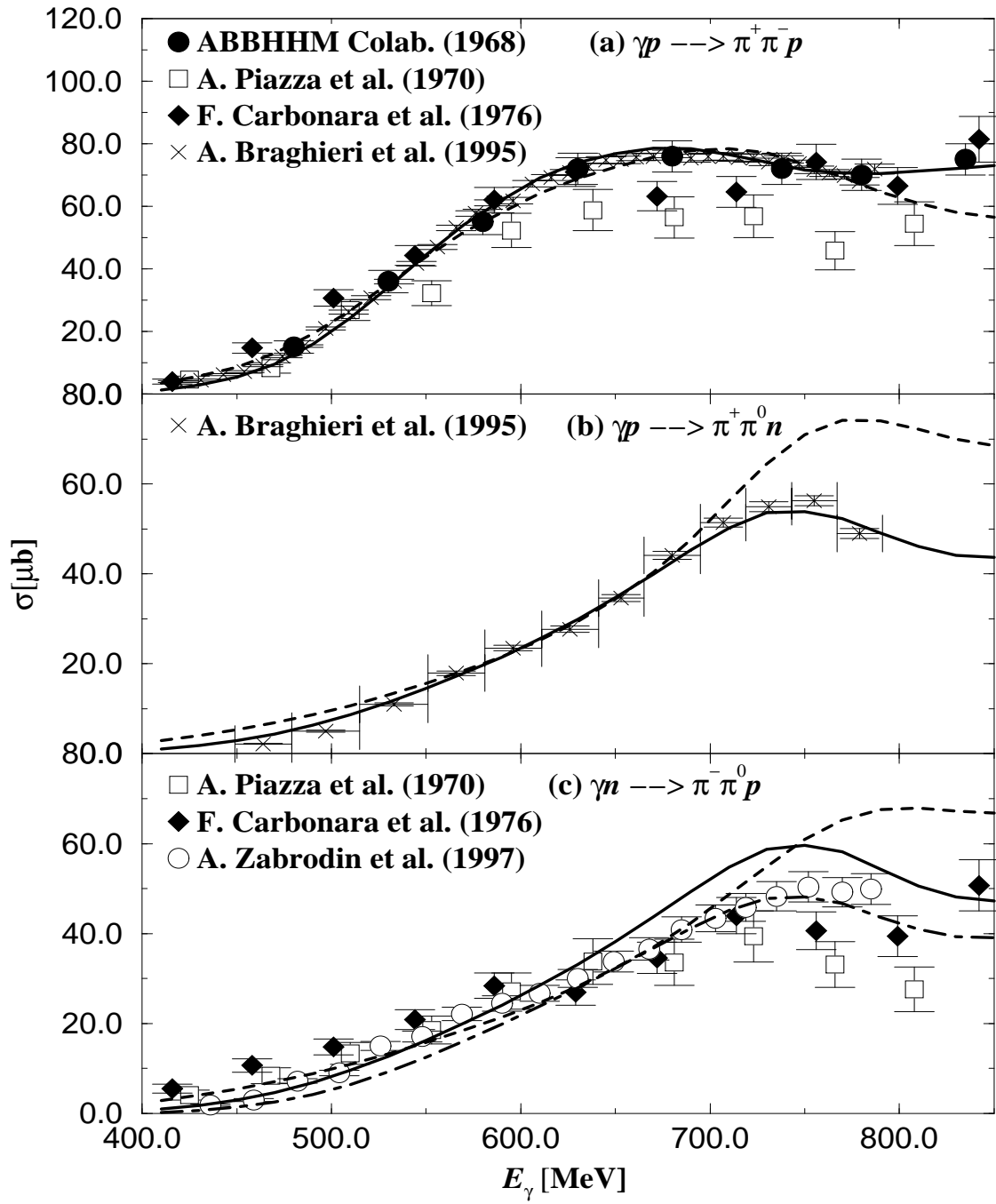


Figure 2

Figure 3

